Connexin32 regulates expansion of liver cancer stem cells via the PI3K/Akt signaling pathway

HONGYU LI[1,2*], BOYING WANG[1,2*], BENQUAN QI[3], GUOJUN JIANG[2], MIN QIN[4] and MEILING YU[1,2]

[1]Department of Pharmacy, The First Affiliated Hospital of Bengbu Medical College; [2]Faculty of Pharmacy, Bengbu Medical College; [3]Department of Emergency Internal Medicine, The First Affiliated Hospital of Bengbu Medical College, Bengbu, Anhui 233004; [4]Department of Pharmacy, Guangdong Provincial People's Hospital, Guangdong Academy of Medical Sciences, Guangzhou, Guangdong 510080, P.R. China

Received April 11, 2022; Accepted June 28, 2022

DOI: 10.3892/or.2022.8381

Abstract. Liver cancer stem cells (LCSCs) are responsible for liver cancer recurrence, metastasis, and drug resistance. Previous studies by the authors demonstrated that upregulated expression of connexin 32 (Cx32) reversed doxorubicin resistance and reduced invasion and metastasis of liver cancer cells. However, the role of Cx32 in expansion of LCSCs remains unclear. A total of 85 patients were enrolled in the present study and followed-up for 5 years. The expression of Cx32 in hepatocellular carcinoma (HCC) tissues and corresponding paracancerous tissues were detected by immunohistochemistry (IHC). Cx32 was silenced in HepG2 cells and overexpressed in HCCLM3 cells and the stemness of liver cells was examined by detecting the expression of LCSC markers (EpCAM, CD133, Nanog, Oct4, Sox9, c-Myc), sphere formation, and xenograft tumorigenesis. Finally, the effect of the phosphoinositide 3-kinase (PI3K)/protein kinase B (Akt) pathway on Cx32-regulated LCSC expansion was investigated. Cx32 was downregulated in LCSCs and HCC tissues, and predicted poor prognosis in patients with HCC. Overexpression of Cx32 in HCCLM3 cells significantly inhibited LCSC expansion, tumorigenesis, and phosphoinositide 3-kinase/protein kinase B (PI3K/Akt) pathway activity. By contrast, silencing of Cx32 in HepG2 cells upregulated expansion of LCSCs and PI3K/Akt pathway activity. Modulating the activity of the PI3K/Akt pathway by SC-79 and LY294002 in HepG2 and HCCLM3 cells, respectively, confirmed that Cx32 could affect the expansion of LCSCs through PI3K/Akt signaling. In conclusion, the present study demonstrated that Cx32 regulated the expansion of LCSCs, and increased expression of Cx32 significantly inhibited the expansion of LCSCs, suggesting that Cx32 may be an optimal target for intervention of HCC.

Correspondence to: Dr Meiling Yu, Department of Pharmacy, The First Affiliated Hospital of Bengbu Medical College, 287 Changhuai Road, Bengbu, Anhui 233004, P.R. China
E-mail: yumeiling409@sohu.com

Dr Min Qin, Department of Pharmacy, Guangdong Provincial People's Hospital, Guangdong Academy of Medical Sciences, 106 Zhongshan Second Road, Guangzhou, Guangdong 510080, P.R. China
E-mail: qinmin23@foxmail.com

*Contributed equally

Key words: connexin 32, PI3K/Akt, hepatocellular carcinoma, cancer stem cell, prognosis

Introduction

Liver cancer is one of the most common malignant tumors worldwide, with the highest incidence in East Asia and Africa, and with the highest prevalence in China (1,2). Hepatocellular carcinoma (HCC) is the main histological type, accounting for approximately 75% of all liver cancers (3). Numerous factors can induce HCC, including viruses (hepatitis B and hepatitis C virus), alcohol consumption, and metabolic disorders (4). Treatment of HCC includes radiotherapy, surgery, and chemotherapy. Even with the use of novel drugs and improved surgical techniques, the mortality rate of patients with HCC remains high due to its high recurrence and metastasis (5). Thus, the mechanisms of HCC recurrence and metastasis need to be determined to improve patient outcome.

Cancer stem cells (CSCs) play a decisive role in tumor initiation and growth, and they are the basis for tumor recurrence, metastasis, and chemotherapy resistance (6). CSCs are a class of heterogeneous cells with stem cell properties and strong tumorigenicity. CSCs can be obtained by screening unique surface markers that include CD133, epithelial cell adhesion molecule (EpCAM), CD73, Sox-9, Nanog, Oct-4, and c-Myc (3,7-9). Previous studies have demonstrated that inhibiting or blocking surface markers of LCSCs can effectively interfere with the self-renewal and proliferation of LCSCs, and reverse cell drug resistance (3,7,8). For example, knockdown of CD73 was revealed to significantly reduce

lenvatinib resistance and tumorigenicity of LCSCs (9), silencing of CD133 was demonstrated to reduce the proliferative capacity of LCSCs (10), and downregulation of EpCAM expression was shown to inhibit the self-renewal and tumorigenicity of LCSCs (11). Thus, targeting LCSCs has become a new strategy to treat liver cancer and improve prognosis (12).

The gap junction is an intercellular protein channel composed of connexins (Cxs). The channel is used for signal exchange, which can inhibit tumors and is involved in overcoming drug resistance in various solid tumors, including breast, lung, and liver cancers (13). During the initiation and progression of liver cancer, the expression level of Cx32 has been revealed to be significantly reduced (14). Previous studies by the authors, demonstrated that upregulating the expression of Cx32 in liver cancer cells could reverse doxorubicin resistance and reduce invasion and metastasis of liver cancer cells (15,16). Trosko *et al* reported that the reason for the emergence of CSCs may be ascribed to the failure of the transcription of Cxs, or abnormal gap junction function related to the post-translational modification of Cxs (17). Based on published studies and previous research by the authors, it is inferred that decreased Cx32 expression induces the expansion of LCSCs, giving rise to enhanced cell invasion, metastasis, and chemotherapeutic drug resistance.

The phosphoinositide 3-kinase/protein kinase B (PI3K/Akt) signaling pathway is important in tumor regulation. Targeting the pathway can effectively inhibit tumor growth. Numerous drugs targeting PI3K signal transduction have entered clinical trials (18). Persistent activation of the PI3K/Akt pathway has been demonstrated to maintain the stemness of CSCs and promote their expansion (19). For instance, activation of PI3K/Akt in colorectal cancer stem cells was shown to promote the migration, invasion, and chemoresistance of spheroid cells (20). In liver cancer, a PI3K/Akt inhibitor was also revealed to reduce the proportion and weaken the expansion capacity of LCSCs (21). In a previous study by the authors, Cx32 was demonstrated to regulate the activity of the PI3K/Akt signaling pathway in liver cancer cells. Overexpression of Cx32 inhibited the PI3K/Akt pathway, while silencing the expression of Cx32 activated the PI3K/Akt pathway (16). Given that LCSCs are the source of tumor initiation, metastasis recurrence, and therapy resistance (22), it is proposed that Cx32 may affect the expansion of HCC stem cells through the PI3K/Akt pathway, thus affecting the malignant phenotypes of HCC cells.

In the present study, 85 patients who underwent radical surgery for liver cancer were followed-up and the association between Cx32 expression and patient survival was analyzed. The Cancer Genome Atlas (TCGA) data was also used to validate the results of the present study. The role of Cx32 in the tumorigenicity of LCSCs was studied in nude mice. It was observed that expansion of LCSCs was altered by modulating the expression of Cx32 *in vitro*. By activating and inhibiting the PI3K/Akt pathway, it was investigated whether the PI3K/Akt pathway mediated the effects of Cx32 on the expansion of LCSCs. The present study explored the mechanisms of Cx32 in the invasion, metastasis, and drug resistance of liver cancer. New targets and prognostic factors for liver cancer were proposed.

Materials and methods

Reagents. HCCLM3 and HepG2 cells were obtained from Shanghai TongBai Biological Technology Co., Ltd., and were authenticated by STR profiling. Dimethyl sulfoxide (DMSO; product no. 276855), SC-79 (product no. 123871) and LY294002 (product no. 528108), antibodies to Cx32 (product no. MAB3069), and secondary antibodies including HRP-conjugated goat anti-rabbit IgG (H + L) (cat. AP307P) and HRP-conjugated goat anti-mouse IgG (H + L) (cat. AP308P) were purchased from Sigma-Aldrich; Merck KGaA. Antibody to Sox-9 (cat. no. PA5-81966) was obtained from Invitrogen; Thermo Fisher Scientific, Inc. Antibodies to phosphorylated (p)-Akt (product code ab81283), total Akt (product code ab8805), EpCAM (product code ab223582), CD133 (product code ab222782), Nanog (product code ab14959), Oct4 (product code ab181557), c-Myc (product code ab32072), β-actin (product code ab8226) were obtained from Abcam. Short hairpin RNA (shRNA)-Cx32 and overexpression (OE)-Cx32 plasmid were obtained from Shanghai GenePharma Co., Ltd.

Patients and tumor samples. The specimens of 85 patients (63 males and 22 females; aged 25-78 years) with liver cancer were collected from the Department of Hepatobiliary Surgery, the First Affiliated Hospital of Bengbu Medical College (Bengbu, China) from January 2014 to December 2015. A total of 124 patients were followed-up to December 2020, but 39 patients were lost to follow-up in the present study. Inclusion criteria were as follows: A pathological diagnosis of liver cancer, complete clinical data records, no history of chemotherapy, radiation, immunotherapy, or other related treatment, no history of other cancers, and no metastases from other organs. The collected specimens included HCC tissues and the corresponding paracancerous tissues. The paracancerous tissues were non-cancerous liver tissues located at least 5 cm from the lesions. This study was approved by the Ethics Committee of Bengbu Medical College (approval no. 2020047).

Western blotting. Proteins of tissues and cells were extracted using a lysis buffer containing a protease inhibitor (product no. P0013B; Beyotime Institute of Biotechnology) and quantified using a BCA protein assay kit (product no. P0012; Beyotime Institute of Biotechnology). Total proteins (20 μg per lane) were separated using 10% SDS-PAGE. The resolved proteins were transferred to a PVDF membrane. The PVDF membrane was then incubated at 4˚C for 1 h with 1X Protein Free Rapid Blocking Buffer (cat. no. PS108P; Shanghai Epizyme Biomedical Technology Co., Ltd.). Following sealing, the membrane was incubated at 4˚C overnight in the corresponding primary antibody solution containing EpCAM (1:1,000), CD133 (1:2,000), Nanog (1:2,000), Oct4 (1:2,000), Sox9 (1:1,000), c-Myc (1:1,000), Cx32 (1:1,000), p-Akt (1:2,000), total Akt (1:1,000), or β-actin (1:1,000). The membrane was washed the following day and incubated with the secondary antibodies, HRP-conjugated goat anti-rabbit IgG or HRP-conjugated goat anti-mouse IgG (1:2,000 or 1:4,000), incubated at 4˚C for 1 h. Finally, the membrane was developed in the dark after incubating with enhanced chemiluminescence reagent (product no. RPN2235; Cytiva). The gray

value of the protein bands was analyzed by ImageJ software [version 1.46r; National Institutes of Health (NIH)].

Immunohistochemistry (IHC). The expression of Cx32 and p-Akt was detected by IHC. Paraffin-embedded specimens were cut into 5 μm-thick slices using a microtome. The tissue sections were dewaxed and hydrated, endogenous peroxidase was inactivated with 3% hydrogen peroxide, antigen repair was performed by microwave irradiation. The tissue sections were blocked at room temperature in 5% bovine serum albumin (BSA)/50 mM PBS (pH 7.4) and incubated with the Cx32 antibody (1:100; product no. MAB3069; Sigma-Aldrich; Merck KGaA) and p-Akt antibody (1:100; product code ab81283; Abcam) at 4˚C overnight. The sections were washed with phosphate-buffered solution and incubated with secondary antibodies, goat anti-mouse IgG HRP conjugate (1:200; product no. 12-349) and goat anti-rabbit IgG HRP conjugate (1:200; product no. 12-348; both from Sigma-Aldrich; Merck KGaA), followed by color development with 3,3' diaminobenzidine (DAB) kit (product no. D3939; Sigma-Aldrich, Merck KGaA), redyeing, dehydration, and sealing. Each section was observed and images were captured using model IX71 optical microscope (Olympus Corporation). All imaged sections stained by immunohistochemistry were analyzed using ImageJ software version 1.46r (NIH). The criteria for staining cells were the same as those previously reported (15).

Spheroid formation assay. Agarose (1%) was spread on a 10-cm cell culture dish and allowed to coagulate. A total of $3x10^5$ cells/ml were plated per well of a gel-coated petri dish and maintained with B27 serum-free microsphere medium (Gibco; Thermo Fisher Scientific, Inc.). N2 (Gibco; Thermo Fisher Scientific, Inc.), 20 ng/ml epidermal growth factor, and 20 ng/ml basic fibroblast growth factor (Invitrogen; Thermo Fisher Scientific, Inc.) were added to DMEM/F12 basal culture medium (Gibco; Thermo Fisher Scientific, Inc.). After 3-4 days, the cells were supplemented with microsphere medium and cultured for another 4-6 days. Images of the spheroids were captured and counted by fluorescence microscope (Olympus Corporation).

Mining of the cancer genome atlas (TCGA) database. TCGA Liver Hepatocellular Carcinoma (LIHC) data were obtained from UCSC Xena (URL: http://xena.ucsc.edu). Screened samples expressed GJB1 (Cx32) and had sufficient survival information. The R language Survival package (https://CRAN.R-project.org/package=survival) was used to evaluate the association between Cx32 expression level and survival outcomes, such as overall survival (OS), disease-free interval (DFI), progression-free interval (PFI), and disease-specific survival (DSS).

Nude mice xenograft tumor model. All animal experiments were conducted in accordance with the regulations approved by the Laboratory Animal Management and Ethics Committee of Bengbu Medical College. A total of 64 male BALB/c mice (4 weeks of age, 20-22 g) were purchased from Beijing Weitong Lihua Experimental Animal Technology Co., Ltd. They were bred in individually ventilated cages (IVC) with specific pathogen-free (SPF) conditions in a 12-h light/dark cycle, 40-70% relative humidity, and controlled temperature (24±2˚C). During the experiment, all mice had free access to standard mice chow and water. Following one-week acclimation, the mice were divided randomly into two groups: HCCLM3 overexpression empty vector (HCCLM3 EV) group and HCCLM3 overexpression (HCCLM3 OE) group. Different numbers of HCC cells ($1x10^3$, $5x10^3$, $1x10^4$, and $5x10^4$) were suspended in Matrigel (50%; BD Biosciences) and injected subcutaneously into the nude mice to observe tumor growth. Finally, the mice were divided into eight groups, with eight mice in each group. Two months later, the mice were euthanized by cervical dislocation under anesthesia (1% pentobarbital sodium, 80 mg/kg, ip) and tumorigenicity of the cells *in vivo* was evaluated. The evaluation criterion was negative if no obvious tumor nodules were found at the injection site of the nude mice. The animal experiments were approved by the Ethics Committee of Bengbu Medical College (approval no. 2020090).

Reverse transcription-quantitative PCR (RT-qPCR). Total RNA of cells was extracted using TRIzol® (cat. no. 15596026; Invitrogen; Thermo Fisher Scientific, Inc.). RNA purity was evaluated by Agilent Bioanalyzer 2100 (Agilent Technologies, Inc.) before RT-qPCR analysis. Subsequently, the cDNA was reverse-transcribed using TaqMan Reverse Transcription reagent (cat. no. N8080234; Invitrogen; Thermo Fisher Scientific, Inc.) according to the manufacturer's protocol, and was detected by fluorescence qPCR using SYBR™ Green PCR Master Mix (cat. no. 4309155; Invitrogen; Thermo Fisher Scientific, Inc.). PCR amplification conditions were as follows: Pre-denaturation at 95˚C for 15 sec, denaturation at 95˚C for 5 sec, and annealing and extension at 62˚C for 30 sec. These steps were repeated for 45 cycles. The absorbance value was read at each extension stage. β-actin was used as the reference gene. The relative gene expression levels of each group were calculated according to quantification cycle (Cq) value (23). Primers of β-actin, Sox-9, CD133, EpCAM, Nanog, Oct4 and c-Myc were obtained from Shanghai Shenggong Biological Technology Co., Ltd. Primers for each gene are listed in Table I.

Cell transfection. Negative control (NC)-shRNA lentivirus and Cx32-shRNA lentivirus were prepared by inserting NC-shRNA and Cx32-shRNA into the respective lentivirus vectors. Lentivirus were produced in 293T cells (Shanghai TongBai Biological Technology Co., Ltd.) using a second generation lentiviral system (Invitrogen; Thermo Fisher Scientific, Inc.). Briefly, $4x10^6$ 293T cells were seeded in a 100-cm culture dish at 24 h before transfection. Subsequently, 6 μg lentiviral construct, 3 μg psPAX2 (packaging plasmid), and 1.5 μg pDM2.G (envoloping plasmid; both from Sangon Biotech Co., Ltd.) were co-transfected into 293T cells (the mixed ratio was pDM2.G: psPAX2: lentivirus, 1:2:4) using Lipofectamine™ 2000 (Invitrogen; Thermo Fisher Scientific, Inc.). Following transfection for 6 h at 37˚C in a CO_2 incubator, the medium was replaced with normal culture medium. After 48 h, the lentivirus-containing supernatants were harvested, centrifuged at 800 x g for 4 min to pellet cell debris. The HepG2 cells were plated at 30-50% confluence, transfected with lentivirus supernatants at a multiplicity of infection (MOI)

Table I. Primers used for quantitative PCR.

Gene name	Primer sequences(5'-3')	
	Forward primer	Reverse primer
β-actin	CATCCACGAAACTACCTTCAACTCC	GAGCCGCCGATCCACACG
Sox-9	AGGAAGTCGGTGAAGAACGG	AAGTCGATAGGGGGCTGTCT
CD133	TGGATGCAGAACTTGACAACGT	ATACCTGCTACGACAGTCGTGGT
EpCAM	CGCAGCTCAGGAAGAATGTG	TGAAGTACACTGGCATTGACGA
Nanog	AATACCTCAGCCTCCAGCAGATG	TGCGTCACACCATTGCTATTCTTC
Oct4	GTGTTCAGCCAAAAGACCATCT	GGCCTGCATGAGGGTTTCT
c-Myc	CCCTCCACTCGGAAGGACTA	GCTGGTGCATTTTCGGTTGT

of 20 TU/ml. A total of 24 h after transfection, the transformed cells were screened by doxycycline (final concentration, 2 μg/ml) for 7-10 days. The transfection results were identified by western blotting. The sequences for the shRNA targeting Cx32 (shCx32) were: shRNA1, 5'-CCGGGCCGTCTTCATGTA TGTCTTTCTCGAGCCCTCACTACATGAAGACGGCTTTTT G-3'; and shRNA2, 5'-CCGGCGTTTGCTATGACCAATTCT TCTCGAGAAGAATTGGTCATAGCAAACGTTTTTG-3'; and the sequence for the NC was: 5'-CCTAAGGTTAAGTCGCCC TCGCTCGAGCGAGGGCGACTTAACCTTAGG-3'.

Statistical analysis. SPSS 23.0 (IBM Corp.) and SigmaPlot 10.0 software (Jandel Corporation; Systat Software, Inc.) were used for statistical analysis. Data represented the mean ± SEM from three independent experiments. Parametric data were analyzed using unpaired t-test or one-way ANOVA with Tukey's multiple comparison test for post hoc comparison. The association between Cx32 expression and clinicopathological characteristics was determined by Pearson χ^2 test. The chi-square test and Fisher's exact probability tests were used as appropriate to evaluate the significance of differences in data between groups. Survival curves were analyzed using the Kaplan-Meier method, and significance was assessed by the Gehan-Breslow-Wilcoxon test or log-rank test. $P<0.05$ was considered to indicate a statistically significant difference.

Results

Cx32 predicts poor prognosis in HCC patients. TCGA data analysis showed that the OS of patients with high expression of Cx32 was significantly higher than those with low expression of Cx32 (Fig. 1A). The same results were observed for the DSS, DFI and PFI (Fig. 1B-D). The data of 85 patients with liver cancer was collected and the expression of Cx32 was assessed in cancer tissues and corresponding paracancerous tissues by IHC. The positive expression rate of Cx32 was 41.2% (35/85) in cancer tissues and 82.4% (70/85) in paracancerous tissues (Fig. 1F). The rate in paracancerous tissue was significantly higher than the rate in cancer tissues. The 85 patients were followed-up for 5 years (Table II). Survival analysis revealed an overall survival rate of 46.39% in the Cx32-positive group and 10.31% in the Cx32-negative group (Fig. 1G; P=0.007), indicating a significant association of Cx32 with prognosis of HCC.

Cx32 expression is downregulated in LCSCs. $CD133^+$ and $EpCAM^+$ liver CSCs, and $CD133^-$ and $EpCAM^-$ non-liver CSCs were sorted from primary HCC tissues. RT-qPCR was used to determine the level of Cx32. Cx32 was significantly reduced in $CD133^+$ and $EpCAM^+$ liver CSCs (Fig. 2A and B). Cx32 mRNA expression was also decreased in HCC spheres derived from human primary HCC cells, compared with adherent cells (Fig. 2C). Consistent with these results, Cx32 was reduced in $CD133^+$ and $EpCAM^+$ liver CSCs sorted from spheres of HepG2 and HCCLM3 cells (Fig. 2D and E). Moreover, compared with the attached cells, Cx32 was obviously decreased in the self-renewing spheroids (Fig. 2F). These results indicated that Cx32 regulated the expansion of LCSCs.

Cx32 regulates the expansion of LCSCs. To explore the effect of Cx32 on the expansion of LCSCs, HepG2 cells (that express a high level of Cx32) and HCCLM3 (that express a low level of Cx32) were used (Fig. 3A and B), and Cx32 was silenced in HepG2 cells and overexpressed in HCCLM3 cells (Fig. 3C-F). RT-qPCR and western blotting were used to observe the expression levels of stemness-associated genes, including EpCAM, CD133, Sox9, Nanog, Oct4, and c-Myc. Self-renewal ability was detected by the spheroid formation assay. Cx32 knockdown in HepG2 cells significantly enhanced the mRNA expression of stemness-associated genes (Fig. 4A), and western blotting results were consistent with those of RT-qPCR (Fig. 4C and D). Moreover, after Cx32 was silenced in HepG2 cells, the numbers of spheres were significantly increased (Fig. 4G and H). By contrast, overexpression of Cx32 in HCCLM3 cells significantly decreased the expression of stemness-associated genes (Fig. 4B, E, and F) and cells formed smaller and fewer spheroids than the control cells (Fig. 4I and J). *In vivo* limiting dilution assay results showed that overexpression of Cx32 markedly downregulated the tumorigenicity capacity of HCCLM3 cells (Fig. 4K-N). Collectively, the results indicated that Cx32 regulated expansion of LCSCs.

Regulation of the PI3K/Akt signaling pathway by Cx32. It was previously confirmed by the authors that Cx32 regulates the PI3K/Akt pathway in HCC (16). In the present study, IHC was used to detect the expression of p-Akt in HCC tissues and corresponding paracancerous tissues. Only 9.4% (8/85)

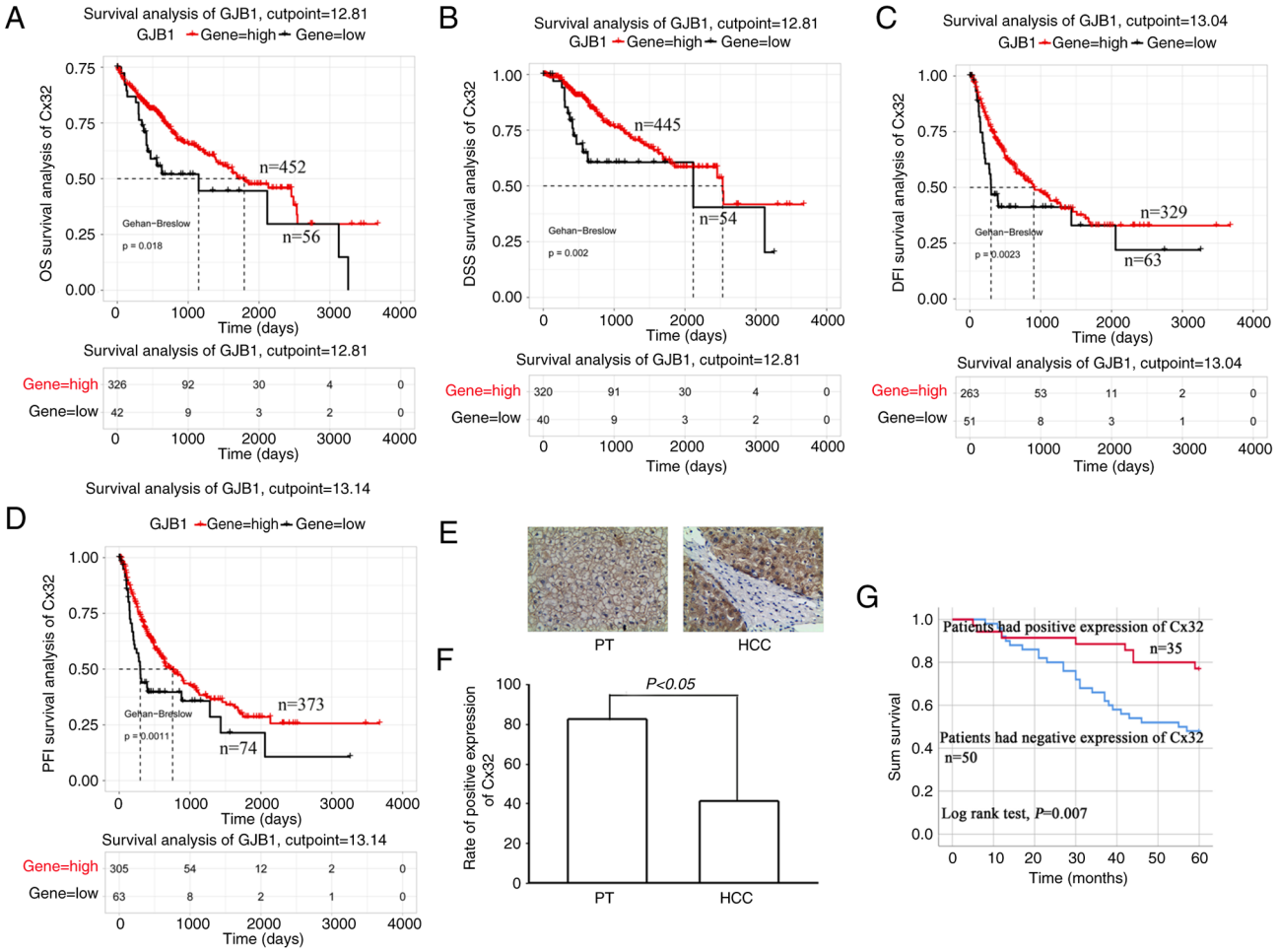

Figure 1. Cx32 predicts poor prognosis in HCC patients. (A-D) Survival analysis of the Cx32 gene in patients with HCC based on TCGA database. Survival is expressed as OS, DSS, DFI and PFI. (E) Immunohistochemical detection of the expression level of Cx32 in HCC specimens and corresponding PT. Magnification, x200. (F) Rate of positive expression of Cx32 in HCC specimens and PT. (G) Kaplan-Meier survival plots for all HCC patients with positive expression of Cx32 and negative expression of Cx32. Log rank testing was used to analyze the data; P<0.05. Cx32, connexin 32; HCC, hepatocellular carcinoma; TCGA, The Cancer Genome Atlas; OS, overall survival; DSS, disease-specific survival; DFI, disease-free interval; PFI, progression-free interval; PT, paracarcinoma tissues.

of patients with HCC had positive expression of p-Akt in the corresponding paracancerous tissues, while the positive expression rate of p-Akt in HCC tissues was 71.8% (61/85) (Fig. 5A and B). The results indicated that p-Akt was activated in HCC tissues. The PI3K/Akt signaling pathway was also activated in HCCLM3 cells. Cx32 was silenced in HepG2 cells and overexpressed in HCCLM3 cells. Western blotting was used to examine PI3K/Akt pathway activity. Cx32 knockdown in HepG2 cells significantly increased the expression level of p-Akt, whereas Cx32 overexpression significantly decreased the expression level of p-Akt (Fig. 5C and D). These findings suggested that Cx32 regulated the activity of the PI3K/Akt signaling pathway in HCC cells.

Cx32 regulates LCSC expansion by the PI3K/Akt signaling pathway. It was next investigated whether Cx32 affected expansion of LCSCs by regulating the PI3K/Akt signaling pathway. HepG2 cells were exposed to the AKT agonist SC-79 to activate the PI3K/Akt signaling pathway. HCCLM3 cells were exposed to the Akt antagonist LY294002 to inhibit the PI3K/Akt pathway. SC-79 significantly enhanced the expression of stemness-associated genes and the numbers of spheres were significantly upregulated (Fig. 6). However, LY294002 obviously decreased the expression of stemness-associated genes, and hepatoma cells formed small and fewer spheroids. The results suggested that PI3K/Akt regulated expansion of LCSCs. In addition, OE-Cx32-HCCLM cells that stably expressed Cx32 were stimulated by the AKT agonist SC-79 and the effect of SC-79 on expansion of LCSCs in these cells was observed. Overexpression of Cx32 in HCCLM3 cells obviously decreased the expression of stemness-associated genes, and cells formed smaller and fewer spheroids, but SC-79 reversed these effects (Fig. 7). These results indicated that Cx32 regulated expansion of LCSCs by the PI3K/Akt signaling pathway.

Discussion

Considering the critical role of LCSCs in tumor initiation, recurrence, metastasis, and drug resistance (22), the mechanisms underlying the expansion of LCSCs need to be comprehensively studied and determined. The present findings from experiments that were performed and from TCGA data demonstrated the positive association between the expression

Table II. Baseline characteristics of 85 patients with HCC.

Clinical characteristics	Variables	No. of patients	Cx32 expression in HCC		P-value
			Positive expression	Negative expression	
Age (years)	≤56	44	22	21	0.061
	>56	41	12	29	
Sex	Female	22	7	15	0.306
	Male	63	27	35	
Alpha-fetoprotein (ng/ml)	≤400	25	10	15	0.0485
	>400	60	24	35	
HBV infection	Yes	51	22	34	0.462
	No	28	12	16	
Liver cirrhosis	Yes	66	28	37	0.325
	No	19	6	13	
Histological differentiation	Poorly	13	6	7	0.559
	Moderately	64	24	39	
	Well	8	4	4	
Tumor capsule	Yes	16	3	13	0.071
	No	69	31	37	
Tumor size (cm)	≤5	46	21	25	0.288
	>5	39	13	25	
Vital status	Deceased	34	16	17	0.236
	Living	51	18	33	
Follow-up time (months)	≤60	34	16	17	0.229
	>60	51	18	33	

HCC, hepatocellular carcinoma; Cx32, connexin 32; HBV, hepatitis B virus.

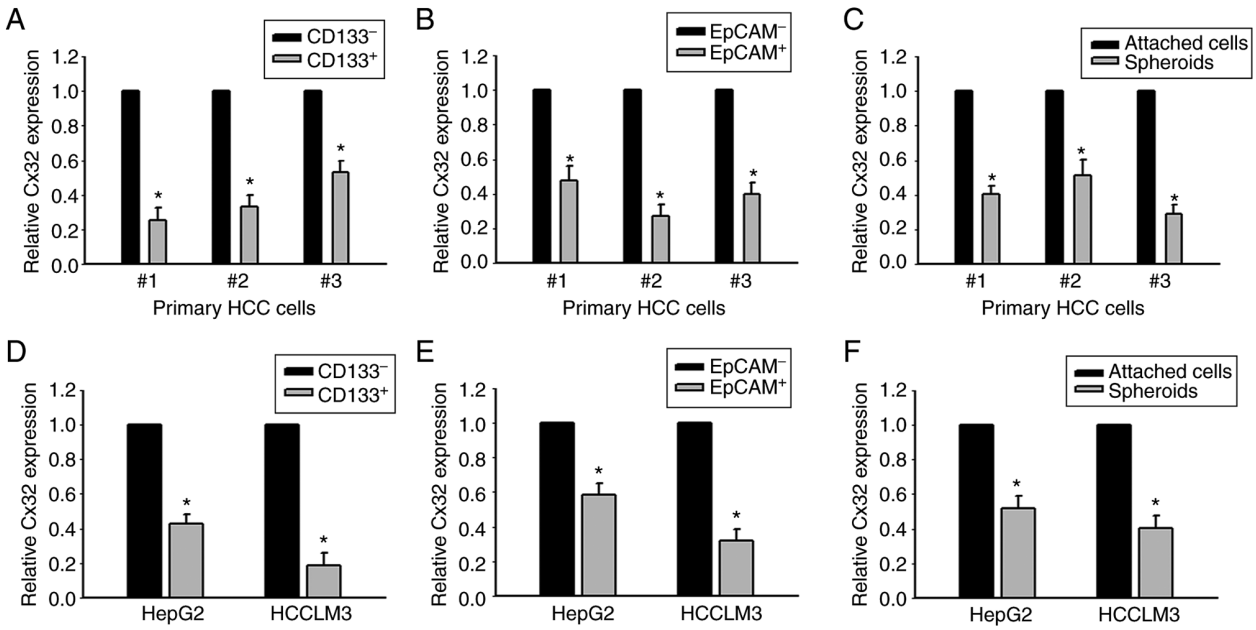

Figure 2. Expression of Cx32 mRNA is decreased in HCC cell populations with higher stem cell characteristics. (A and B) Cx32 mRNA in CD133$^+$, EpCAM$^+$ liver CSCs and CD133$^-$, EpCAM-non-liver CSCs sorted from primary HCC cells was analyzed by qPCR. *P<0.05 vs. the CD133$^-$ or EpCAM$^-$ group. (C) Cx32 mRNA in HCC spheres and attached cells obtained from primary HCC cells was detected by qPCR, *P<0.05 vs. the attached cells. (D and E) Expression level of Cx32 in CD133$^+$, EpCAM$^+$ liver CSCs and CD133$^-$, EpCA$^-$ non-liver CSCs sorted from spheres of HepG2 and HCCLM3 cells was analyzed by qPCR. *P<0.05 vs. the CD133$^-$ or EpCAM$^-$ group. (F) Cx32 mRNA levels were detected in spheres of HepG2 and HCCLM3 cells and corresponding adherent cells. *P<0.05 vs. the attached cells. Cx32, connexin 32; HCC, hepatocellular carcinoma; EpCAM, epithelial cell adhesion molecule; CSCs, cancer stem cells; qPCR, quantitative PCR.

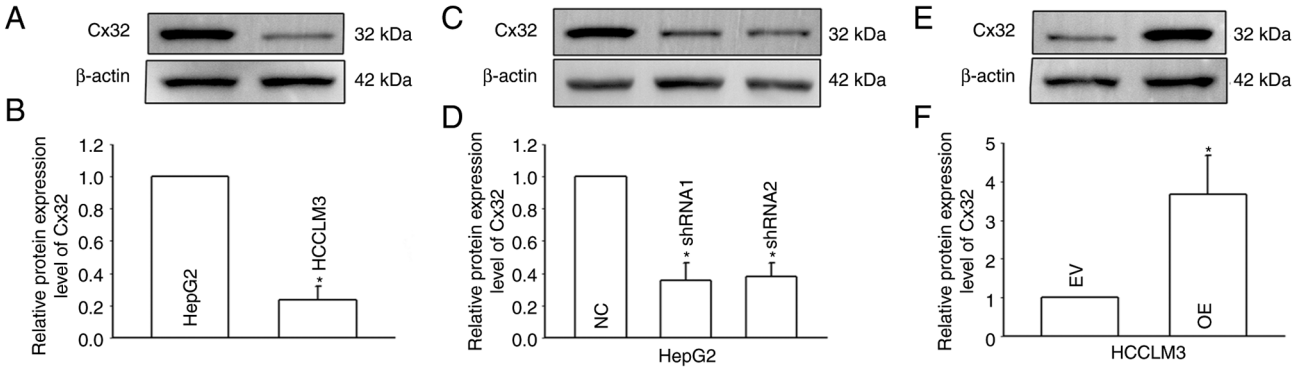

Figure 3. Inhibition of Cx32 expression with shRNA-Cx32 in HepG2 cells, and overexpression of Cx32 in HCCLM3 cells. (A and B) Expression level of Cx32 examined by western blotting in HepG2 and HCCLM3 cells. Results represent the mean ± SEM from three independent experiments; *P<0.05 vs. the HepG2 group. (C and D) Inhibition of Cx32 expression with shRNA-Cx32 in HepG2 cells. (E and F) Overexpression of Cx32 in HCCLM3 cells. Results represent the mean ± SEM from three independent experiments; *P<0.05 vs. the NC group or EV group. The proteins were normalized with β-actin. Cx32, connexin 32; shRNA, small interfering RNA; NC, negative control; EV, empty vector.

level of Cx32 and the prognosis of liver cancer. Moreover, *in vitro* and *in vivo* data indicated that upregulating the expression of Cx32 inhibited the expansion of LCSCs, which was mediated by downregulated activity of the PI3K/Akt pathway. These novel findings revealed a potential mechanism by which Cx32 regulated the expansion of LCSCs.

A total of 85 patients with liver cancer were followed-up for 5 years after radical surgery. In these patients, low expression of Cx32 predicted a worse overall survival. This finding was validated by TCGA data. In addition, TCGA data revealed that high expression of Cx32 was associated with improved DSS, DFI, and PFI compared with low expression of Cx32. These findings implicated Cx32 as a prognostic biomarker for liver cancer.

Cx32 is a Cx that is mainly expressed in hepatocytes. A previous study by the authors confirmed that Cx32 reverses doxorubicin resistance by inhibiting the epithelial-mesenchymal transition (EMT) of HCC cells, and reduces the invasion and metastatic ability of HCC cells (15). EMT is a process in which epithelial cells are transformed to mesenchymal cells with a high migration potential, which promotes the formation of CSCs and maintains their stemness (24). EMT results in enhanced tumor cell invasion, metastasis, and acquisition of drug resistance (25). Dormant tumor cells undergoing EMT can acquire a CSC-like phenotype and facilitate metastasis and proliferation (26). The previous study by the authors revealed that silencing the expression of Cx32 in HepG2 cells induced EMT of liver cancer cells (15). Thus, it was hypothesized that downregulation of Cx32 expression may promote the expansion maintain stemness of LCSCs. In the present study, the expression level of Cx32 in LCSCs was significantly decreased compared with non-LCSCs. Furthermore, compared with attached cells, Cx32 was obviously decreased in the self-renewing spheroids. The previous and present findings suggest that Cx32 may regulate LCSC expansion.

Kawasaki *et al* reported that Cx32 promotes the expansion of LCSCs when translocated from the cell membrane to the cytoplasm (27). During the initiation and development of HCC, the total expression level of Cx32 is significantly reduced and Cx32 is internalized by being translocated from the cell membrane to the cytoplasm (14). The results of IHC confirmed that Cx32 was mainly located in the cytoplasm in liver cancer cells. When the expression of Cx32 was silenced in HepG2 cells, the mRNA and protein levels of liver cancer stemness-related genes CD133, EpCAM, CD73, Sox-9, Nanog, Oct-4, and c-Myc were all significantly upregulated. In addition, the number of spheroids was also increased, indicating enhanced expansion of LCSCs. By contrast, the overexpression of Cx32 in HCCLM3 cells significantly inhibited the expansion of LCSCs *in vitro* and *in vivo*. The present and previous results by the authors support the theory that Cx32 may regulate the expansion of LCSCs in either a channel-related, in which Cx32 located in the cell membrane to form a gap junction channel is downregulated, or in a non-channel-related manner, involving upregulation of Cx32 located in the cytoplasm (27). The results of the present study demonstrated that restoring Cx expression and rebuilding the gap junction is an important strategy to inhibit the expansion of LCSCs.

Gap junctions are dynamic protein channels, and functional gap junctions on the membrane are constantly 'eliminated' through endocytosis and degradation by lysosomes, and are replaced by newly synthesized Cxs (28). Cells modulate the rate of Cx degradation according to the microenvironment, thereby altering the protein channels in the membrane (28,29). Acetylation and ubiquitination of Cx32 are the main factors determining the turnover rate of Cx32. Acetylation stabilizes Cx32 and ubiquitination promotes the degradation of Cx32. Cx32 acetylation may negatively regulate its ubiquitination (30). The effects of acetylation and ubiquitination of Cx32 on the expansion of LCSCs will next be studied, to develop new strategies to inhibit the expansion of LCSCs.

Cx32 regulates the PI3K/Akt signaling pathway in liver cancer cells (16). Activation of the PI3K/Akt signaling pathway strengthens the stemness of CSCs (31-33) and induces drug resistance (32). Therefore, in the present study, the role of the PI3K/Akt signaling pathway in the regulation of the expansion of LCSCs by Cx32 was investigated. The expression of p-Akt in liver cancer tissues was detected and it was determined that the PI3K/Akt pathway was continuously activated in liver cancer tissues compared with adjacent tissues. It was further demonstrated that Cx32 decreased the expansion of LCSCs by

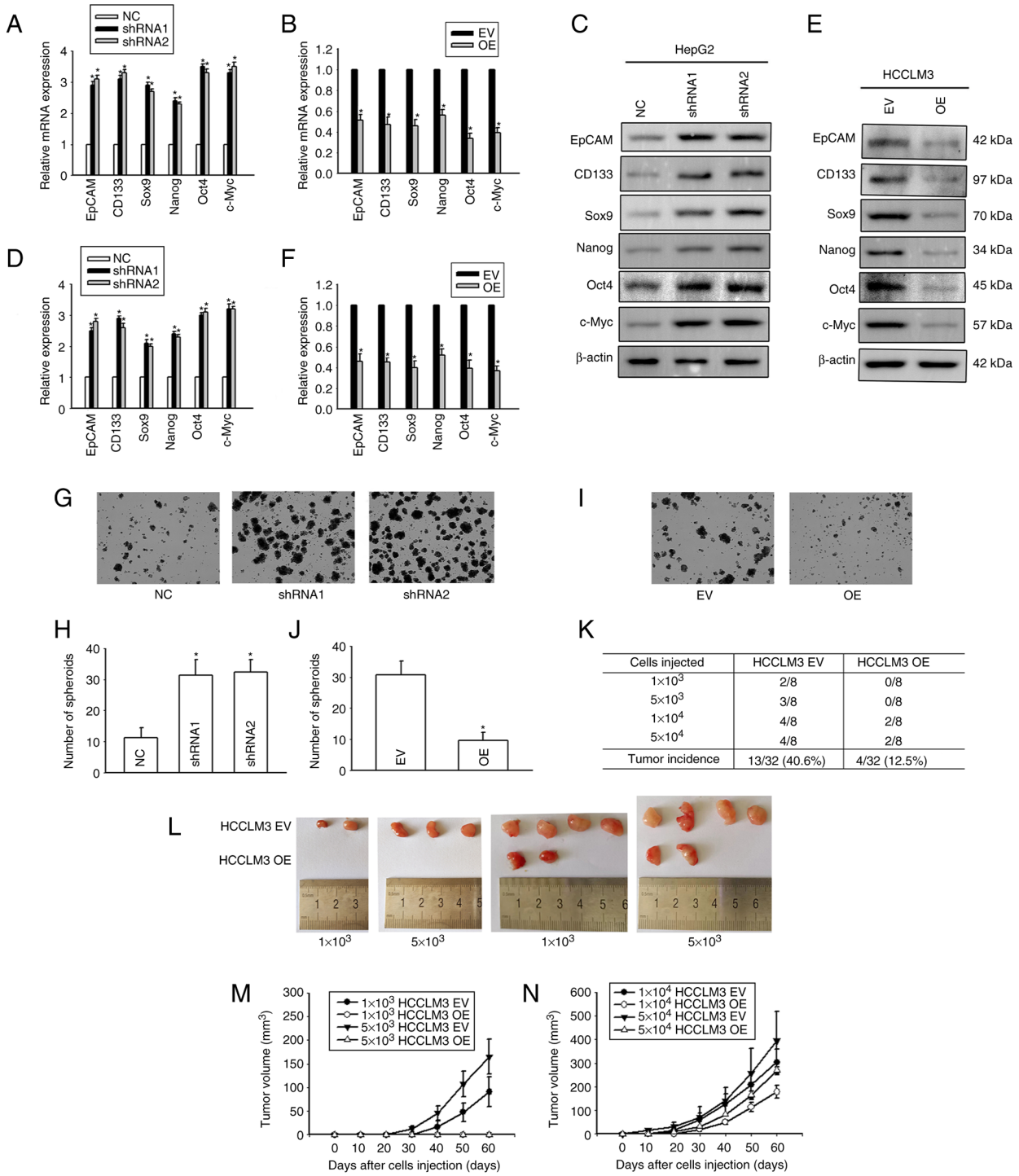

Figure 4. Cx32 regulates the expansion of LCSCs. (A) Effect of Cx32 knockdown on the mRNA expression levels of stemness-associated genes in HepG2 cells. (B) Effect of Cx32 overexpression on the mRNA expression levels of stemness-associated genes in HCCLM3 cells. (C and D) The expression levels of stemness-associated genes were examined by western blotting when HepG2 cells were transfected with shRNA-Cx32. The proteins were normalized with β-actin. (E and F) The expression levels of stemness-associated genes were observed when HCCLM3 cells overexpressed Cx32. The proteins were normalized with β-actin. (G and H) Effect of Cx32 knockdown on the sphere-forming capacities of HepG2 cells. Magnification, x200. The bar graph shows the average number of spheres >100 μm in diameter. (I and J) Effect of Cx32 overexpression on the sphere-forming capacities of HCCLM3 cells. Magnification, x200. The bar graph shows the average number of spheres >100 μm in diameter. For the aforementioned images, the error bars represent the mean ± SEM of three independent experiments; *P<0.05 vs. the NC group; or *P<0.05 vs. the overexpression EV group. (K and L) Efficiency of tumor formation of Cx32 overexpression in HCCLM3 cells. (M) Efficiency of tumor formation of HCCLM3 EV and HCCLM3 OE cells; number of injected cells: $1x10^3$ and $5x10^3$, n=8. (N) Efficiency of tumor formation of HCCLM3 EV and HCCLM3 OE cells; number of injected cells: $1x10^4$, $5x10^4$, n=8. Cx32, connexin 32; LCSCs, liver cancer stem cells; shRNA, small interfering RNA; NC, negative control; EV empty vector; OE, overexpression; EpCAM, epithelial cell adhesion molecule.

inhibiting the activity of the PI3K/Akt pathway *in vitro*. These results shed light on the potential of Cx32 and PI3K/Akt as targets against liver cancer and drug resistance. PI3K/Akt maintains the stemness of CSCs and promotes their expansion by mTOR, NF-κB, or SOX2 (34-36). It was previously confirmed that Cx32 inhibits PI3K/Akt/NF-κB pathway activity in HCC (16). The

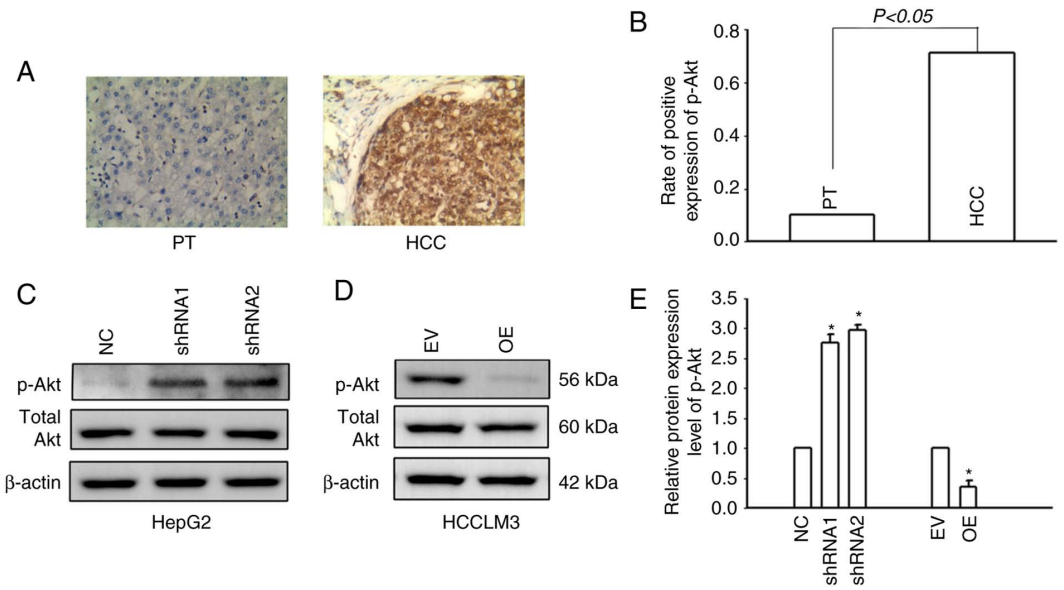

Figure 5. Cx32 modulates the PI3K/Akt signaling pathway. (A) Expression level of p-Akt in HCC tissues and adjacent non-tumorous liver samples assessed by immunohistochemistry. (B) Rate of positive expression of p-Akt in HCC samples and corresponding paracarcinoma tissues. (C) Expression of p-Akt and total Akt examined by western blotting following transfection of HepG2 cells with shRNA-Cx32. (D) Expression of p-Akt and total Akt when HCCLM3 cells were overexpressed with Cx32. (E) Results represent the mean ± SEM from three independent experiments; *P<0.05 vs. the NC group or EV group. The proteins were normalized with β-actin. Cx32, connexin 32; PI3K/Akt, phosphoinositide 3-kinase/protein kinase B; p-, phosphorylated; HCC, hepatocellular carcinoma; shRNA, small interfering RNA; NC, negative control; EV, empty vector; PT, paracarcinoma tissues.

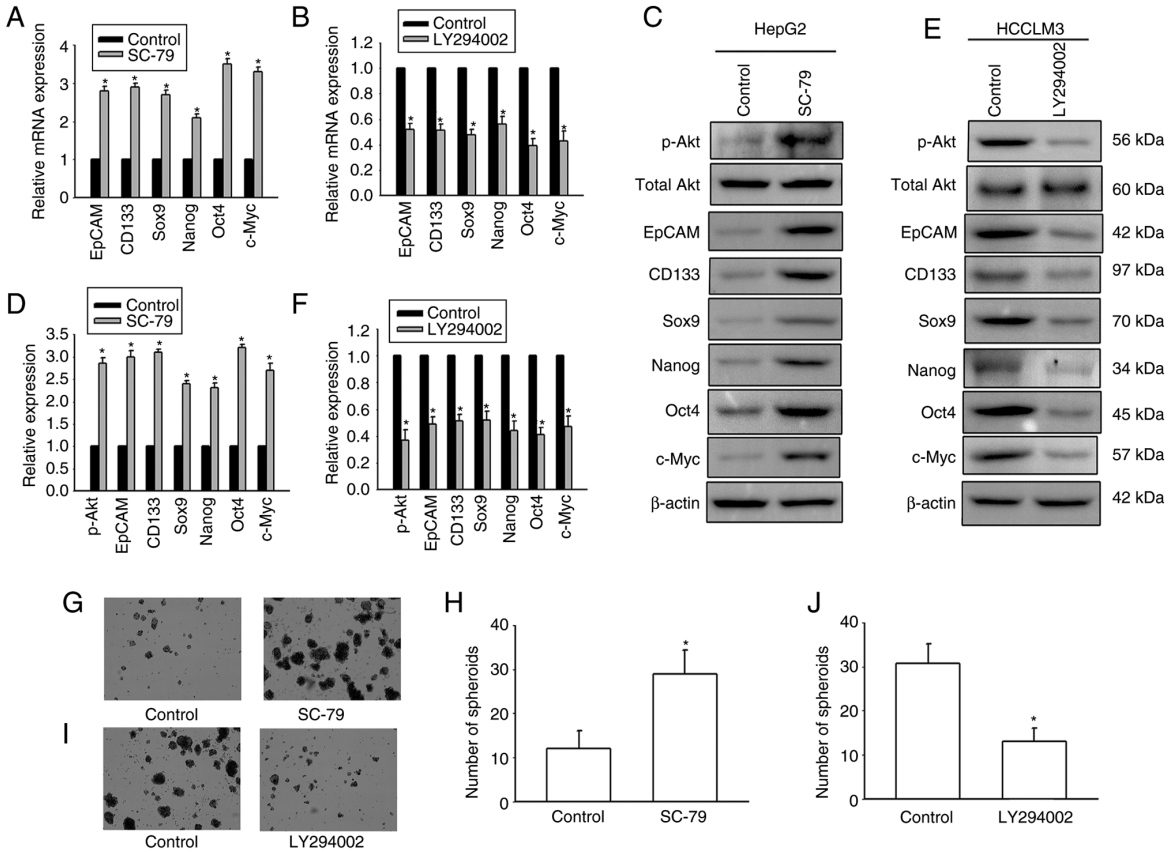

Figure 6. PI3K/Akt signaling pathway modulates the expansion of LCSCs. (A) SC-79 increased the mRNA expression of stemness-associated genes in HepG2 cells. (B) LY294002 decreased the mRNA expression of stemness-associated genes in HCCLM3 cells. (C and D) Effects of SC-79 on the expression levels of stemness-associated genes in HepG2 cells. The proteins were normalized with β-actin. (E and F) Effects of LY294002 on the expression levels of stemness-associated genes in HCCLM3 cells. The proteins were normalized with β-actin. (G and H) Effects of SC-79 on the sphere-forming capacities of HepG2 cells. Magnification, x200. The bar graph shows the average number of spheres >100 μm in diameter. (I and J) Effects of LY294002 on the sphere-forming capacities of HCCLM3 cells. Magnification, x200. The bar graph shows the average number of spheres >100 μm in diameter. All error bars represent the means ± SEM of three independent experiments; *P<0.05 vs. the control group. PI3K/Akt, phosphoinositide 3-kinase/protein kinase B; LCSCs, liver cancer stem cells; EpCAM, epithelial cell adhesion molecule; p-, phosphorylated.

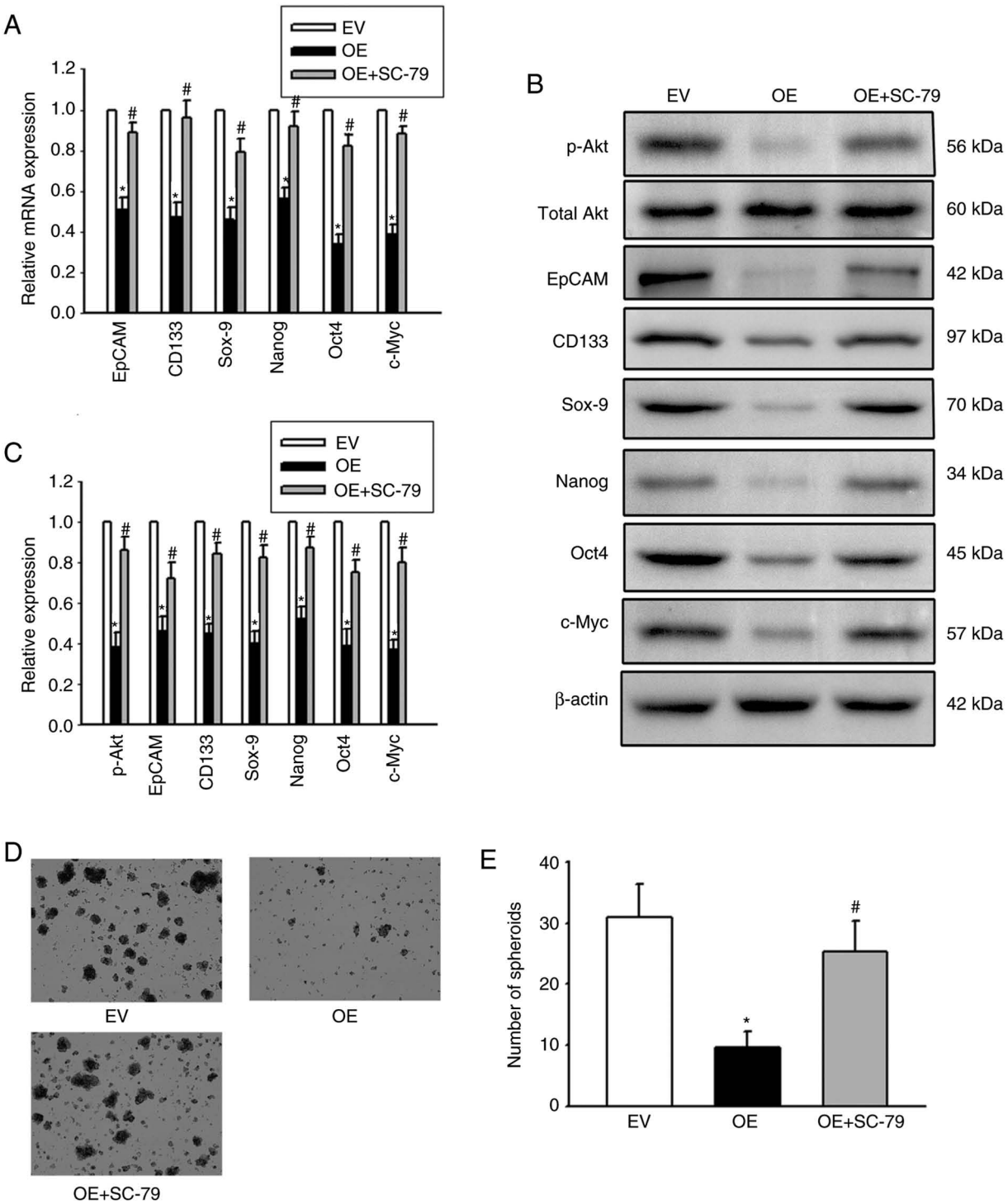

Figure 7. Cx32 regulates the expansion of LCSCs by the PI3K/Akt signaling pathway. (A) Cx32-overexpressing HCCLM3 cells were exposed to SC-79 and the mRNA levels of stemness-associated genes were detected by quantitative PCR. (B and C) The protein levels of stemness-associated genes and PI3K/Akt pathway activity were assessed by western blotting. The proteins were normalized with β-actin. (D and E) The sphere-forming capacities were observed. Magnification, x200. The bar graph shows the average number of spheres >100 μm in diameter. All error bars represent the mean ± SEM of three independent experiments; *P<0.05 vs. the EV group; and $^{\#}$P<0.05 vs. the OE group. Cx32, connexin 32; LCSCs, liver cancer stem cells; PI3K/Akt, phosphoinositide 3-kinase/protein kinase B; EV, empty vector; OE, overexpression; EpCAM, epithelial cell adhesion molecule; p-, phosphorylated.

investigation of whether PI3K/Akt/mTOR, PI3K/Akt/NF-κB, and/or PI3K/Akt/SOX2 pathways are involved in Cx32-regulated expansion of LCSCs, is planned in a future study.

In conclusion, the low expression of Cx32 was associated with a worse prognosis for liver cancer. This association needs to be validated in cohorts involving a larger number of patients. A strategy to inhibit the expansion of LCSCs by recovering the expression of Cx32, was also proposed. In addition, the data illustrated the key role of PI3K/Akt in the regulation of the expansion of LCSCs by Cx32. The present study provided experimental evidence that targeting Cx32 potentially inhibits the invasion and metastasis of liver cancer cells and reverses drug resistance.

Acknowledgements

We would like to thank Mrs Yingying Huang (Department of Pharmacy, The First Affiliated Hospital of Bengbu Medical College) for revising the manuscript.

Funding

The present study was supported by the National Natural Science Foundation of Anhui (grant nos. 1908085MH293 and 1808085QH269), the 512 Talent Cultivation Plan Foundation of Bengbu Medical College (grant no. by51201320), the Natural Science Foundation of the Provincial Education Department of Anhui (grant no. KJ2021A0689), and the Foundation of Bengbu Medical College (grant no. 2020byzd089).

Availability of data and materials

The datasets used and analyzed during the current study are available from the corresponding author on reasonable request.

Authors' contributions

HL performed the *in vitro* study, collected the liver cancer tissues and paracancerous tissues, and wrote the manuscript. BW performed the *in vitro* study and also collected the liver cancer tissues and paracancerous tissues. BQ performed the animal study. GJ analyzed the data and constructed the graphs. MQ designed the study and revised the manuscript. MY designed the study, wrote the manuscript, and revised the manuscript. HL and BW confirm the authenticity of all the raw data. All authors read and approved the final version of the manuscript.

Ethics approval and consent to participate

Ethics approval (approval no. 2020047) was obtained from the Ethics Committee of Bengbu Medical College (Bengbu, China) and written informed consent was obtained from each patient. The animal experiments were approved (approval no. 2020090) by the Ethics Committee of Bengbu Medical College.

Patient consent for publication

Not applicable.

Competing interests

The authors declare that they have no competing financial interests or personal relationships that could have influenced the research reported in the present study.

References

1. Llovet JM, Kelley RK, Villanueva A, Singal AG, Pikarsky E, Roayaie S, Lencioni R, Koike K, Zucman-Rossi J and Finn RS: Hepatocellular carcinoma. Nat Rev Dis Primers 7: 6, 2021.
2. McGlynn KA, Petrick JL and El-Serag HB: Epidemiology of hepatocellular carcinoma. Hepatology 73 (Suppl 1): S4-S13, 2021.
3. Liu YC, Yeh CT and Lin KH: Cancer stem cell functions in hepatocellular carcinoma and comprehensive therapeutic strategies. Cells 9: 1331, 2020.
4. Pinheiro PS, Medina HN, Callahan KE, Jones PD, Brown CP, Altekruse SF, McGlynn KA and Kobetz EN: The association between etiology of hepatocellular carcinoma and race-ethnicity in Florida. Liver Int 40: 1201-1210, 2020.
5. Yang A, Ju W, Yuan X, Han M, Wang X, Guo Z, Wei X, Wang D, Zhu X, Wu L and He X: Comparison between liver resection and liver transplantation on outcomes in patients with solitary hepatocellular carcinoma meeting UNOS criteria: A population-based study of the SEER database. Oncotarget 8: 97428-97438, 2017.
6. Zhou G, Latchoumanin O, Bagdesar M, Hebbard L, Duan W, Liddle C, George J and Qiao L: Aptamer-based therapeutic approaches to target cancer stem cells. Theranostics 7: 3948-3961, 2017.
7. Lan X, Wu YZ, Wang Y, Wu FR, Zang CB, Tang C, Cao S and Li SL: CD133 silencing inhibits stemness properties and enhances chemoradiosensitivity in CD133-positive liver cancer stem cells. Int J Mol Med 31: 315-324, 2013.
8. Karagonlar ZF, Akbari S, Karabicici M, Sahin E, Avci ST, Ersoy N, Ates KE, Balli T, Karacicek B, Kaplan KN, *et al*: A novel function for KLF4 in modulating the de-differentiation of $EpCAM^-$/CD133-nonStem Cells into $EpCAM^+$/$CD133^+$ liver cancer stem cells in HCC cell line HuH7. Cells 9: 1198, 2020.
9. Ma XL, Hu B, Tang WG, Xie SH, Ren N, Guo L and Lu RQ: CD73 sustained cancer-stem-cell traits by promoting SOX9 expression and stability in hepatocellular carcinoma. J Hematol Oncol 13: 11, 2020.
10. Jang JW, Song Y, Kim SH, Kim JS, Kim KM, Choi EK, Kim J and Seo HR: CD133 confers cancer stem-like cell properties by stabilizing EGFR-AKT signaling in hepatocellular carcinoma. Cancer Lett 389: 1-10, 2017.
11. Deng Y, Li M, Zhuo M, Guo P, Chen Q, Mo P, Li W and Yu C: Histone demethylase JMJD2D promotes the self-renewal of liver cancer stem-like cells by enhancing EpCAM and Sox9 expression. J Biol Chem 296: 100121, 2021.
12. Huang B, Yan X and Li Y: Cancer stem cell for tumor therapy. Cancers (Basel) 13: 4814, 2021.
13. Wu JI and Wang LH: Emerging roles of gap junction proteins connexins in cancer metastasis, chemoresistance and clinical application. J Biomed Sci 26: 8, 2019.
14. Nakashima Y, Ono T, Yamanoi A, El-Assal ON, Kohno H and Nagasue N: Expression of gap junction protein connexin32 in chronic hepatitis, liver cirrhosis, and hepatocellular carcinoma. J Gastroenterol 39: 763-768, 2004.
15. Yu M, Han G, Qi B and Wu X: Cx32 reverses epithelial-mesenchymal transition in doxorubicin-resistant hepatocellular carcinoma. Oncol Rep 37: 2121-2128, 2017.
16. Yu M, Zou Q, Wu X, Han G and Tong X: Connexin 32 affects doxorubicin resistance in hepatocellular carcinoma cells mediated by Src/FAK signaling pathway. Biomed Pharmacother 95: 1844-1852, 2017.
17. Trosko JE: Cancer prevention and therapy of two types of gap junctional intercellular communication-deficient 'cancer stem cell'. Cancers (Basel) 11: 87, 2019.
18. Yang J, Nie J, Ma X, Wei Y, Peng Y and Wei X: Targeting PI3K in cancer: Mechanisms and advances in clinical trials. Mol Cancer 18: 26, 2019.
19. Sun S, Xue D, Chen Z, Ou-Yang Y, Zhang J, Mai J, Gu J, Lu W, Liu X, Liu W, *et al*: R406 elicits anti-Warburg effect via Syk-dependent and -independent mechanisms to trigger apoptosis in glioma stem cells. Cell Death Dis 10: 358, 2019.
20. Mangiapane LR, Nicotra A, Turdo A, Gaggianesi M, Bianca P, Di Franco S, Sardina DS, Veschi V, Signore M, Beyes S, *et al*: PI3K-driven HER2 expression is a potential therapeutic target in colorectal cancer stem cells. Gut 71: 119-128, 2022.
21. Kahraman DC, Kahraman T and Cetin-Atalay R: Targeting PI3K/Akt/mTOR pathway identifies differential expression and functional role of IL8 in liver cancer stem cell enrichment. Mol Cancer Ther 18: 2146-2157, 2019.
22. Wang N, Wang S, Li MY, Hu BG, Liu LP, Yang SL, Yang S, Gong Z, Lai PBS and Chen GG: Cancer stem cells in hepatocellular carcinoma: An overview and promising therapeutic strategies. Ther Adv Med Oncol 10: 1758835918816287, 2018.
23. Livak KJ and Schmittgen TD: Analysis of relative gene expression data using real-time quantitative PCR and the 2(-Delta Delta C(T)) method. Methods 25: 402-408, 2001.
24. Shibue T and Weinberg RA: EMT, CSCs, and drug resistance: The mechanistic link and clinical implications. Nat Rev Clin Oncol 14: 611-629, 2017.

25. Tanabe S, Quader S, Cabral H and Ono R: Interplay of EMT and CSC in cancer and the potential therapeutic strategies. Front Pharmacol 11: 904, 2020.
26. Weidenfeld K, Schif-Zuck S, Abu-Tayeh H, Kang K, Kessler O, Weissmann M, Neufeld G and Barkan D: Dormant tumor cells expressing LOXL2 acquire a stem-like phenotype mediating their transition to proliferative growth. Oncotarget 7: 71362-71377, 2016.
27. Kawasaki Y, Omori Y, Li Q, Nishikawa Y, Yoshioka T, Yoshida M, Ishikawa K and Enomoto K: Cytoplasmic accumulation of connexin32 expands cancer stem cell population in human HuH7 hepatoma cells by enhancing its self-renewal. Int J Cancer 128: 51-62, 2011.
28. Totland MZ, Rasmussen NL, Knudsen LM and Leithe E: Regulation of gap junction intercellular communication by connexin ubiquitination: Physiological and pathophysiological implications. Cell Mol Life Sci 77: 573-591, 2020.
29. Jiang JX and Penuela S: Connexin and pannexin channels in cancer. BMC Cell Biol 17 (Suppl 1): S12, 2016.
30. Alaei SR, Abrams CK, Bulinski JC, Hertzberg EL and Freidin MM: Acetylation of C-terminal lysines modulates protein turnover and stability of Connexin-32. BMC Cell Biol 19: 22, 2018.
31. Bamodu OA, Chang HL, Ong JR, Lee WH, Yeh CT and Tsai JT: Elevated PDK1 expression drives PI3K/AKT/mTOR signaling promotes radiation-resistant and dedifferentiated phenotype of hepatocellular carcinoma. Cells 9: 746, 2020.
32. Deng J, Bai X, Feng X, Ni J, Beretov J, Graham P and Li Y: Inhibition of PI3K/Akt/mTOR signaling pathway alleviates ovarian cancer chemoresistance through reversing epithelial-mesenchymal transition and decreasing cancer stem cell marker expression. BMC Cancer 19: 618, 2019.
33. Wu Y, Zhang J, Zhang X, Zhou H, Liu G and Li Q: Cancer Stem Cells: A potential breakthrough in HCC-targeted therapy. Front Pharmacol 11: 198, 2020.
34. Xia P and Xu XY: PI3K/Akt/mTOR signaling pathway in cancer stem cells: From basic research to clinical application. Am J Cancer Res 5: 1602-1609, 2015.
35. Erdogan S, Doganlar O, Doganlar ZB, Serttas R, Turkekul K, Dibirdik I and Bilir A: The flavonoid apigenin reduces prostate cancer CD44(+) stem cell survival and migration through PI3K/Akt/NF-κB signaling. Life Sci 162: 77-86, 2016.
36. Park JH, Kim YH, Shim S, Kim A, Jang H, Lee SJ, Park S, Seo S, Jang WI, Lee SB and Kim MJ: Radiation-activated PI3K/AKT pathway promotes the induction of cancer stem-like cells via the upregulation of SOX2 in colorectal cancer. Cells 10: 135, 2021.